SUPPLEMENTARY FIGURES

Wade et al, "The Snf1 kinase and the proteasome-associated Rad23 regulate UV-responsive gene expression."

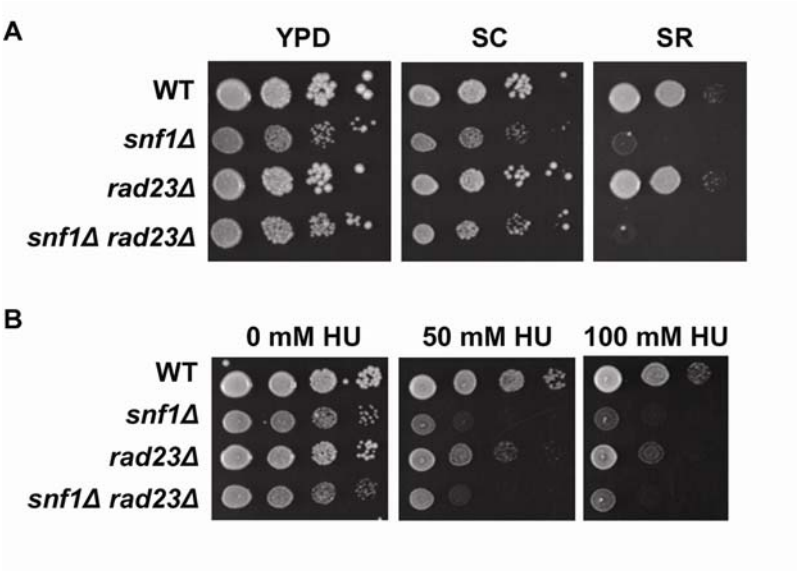

Figure S1: *SNF1-RAD23* genetic interaction is specific to UV irradiation.

(A) 10-fold serial dilutions of yeast cultures were spotted onto YPD, synthetic complete media containing 2% glucose (SC) and synthetic media containing 2% raffinose (SR). There was no synthetic growth defect of *snf1Δ rad23Δ* cells under these conditions.

(B) 10-fold serial dilutions of yeast cultures were spotted onto YPD containing the indicated concentration of hydroxyurea (HU). Deletion of *RAD23* did not enhance the HU sensitivity of *snf1*Δ cells.

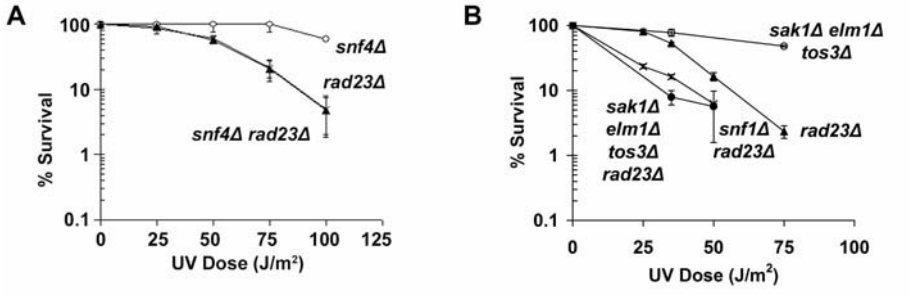

Figure S2: Snf1 activation is important for UV resistance.

(A) UV survival curve of the indicated yeast strains. Results were obtained as in Figure 3A. Unlike deletion of the catalytic subunit, deletion of *SNF4,* encoding the regulatory subunit of the Snf1 kinase complex, had no effect on UV sensitivity of *rad23Δ* cells. This further supports the idea that low level basal kinase activity is important for UV resistance whereas activation of Snf1 kinase is not critical under these conditions.

(B) UV survival curve for the indicated strains; the experiment was performed as in Figure 3A. Three kinases activate Snf1 in *Saccharomyces cerevisiae,* encoded by *ELM1, TOS3* and *SAK1* (Hong et al, 2003; Sutherland et al, 2003). Deletion of each of these separately had no effect on the UV sensitivity of either WT or *rad23Δ* cells (data not shown). Loss of all three kinases was required for loss of Snf1 activity in response to glucose deprivation (Hong et al, 2003). Deletion of *ELM1, TOS3* and *SAK1* in *rad23Δ* cells resulted in UV sensitivity comparable to deletion of *SNF1* itself. This indicates that the same upstream kinases that are responsible for Snf1 activation during glucose starvation also function redundantly in response to UV irradiation. Since the UV sensitivity of the quadruple mutant here is different from that of the *snf1-T210A* mutant (Figure 3C), it also suggests that these three kinases may have additional targets that contribute to UV resistance in *rad23Δ* cells. In both panels, the error bars represent the standard deviation of the mean for cells plated and irradiated in triplicate.

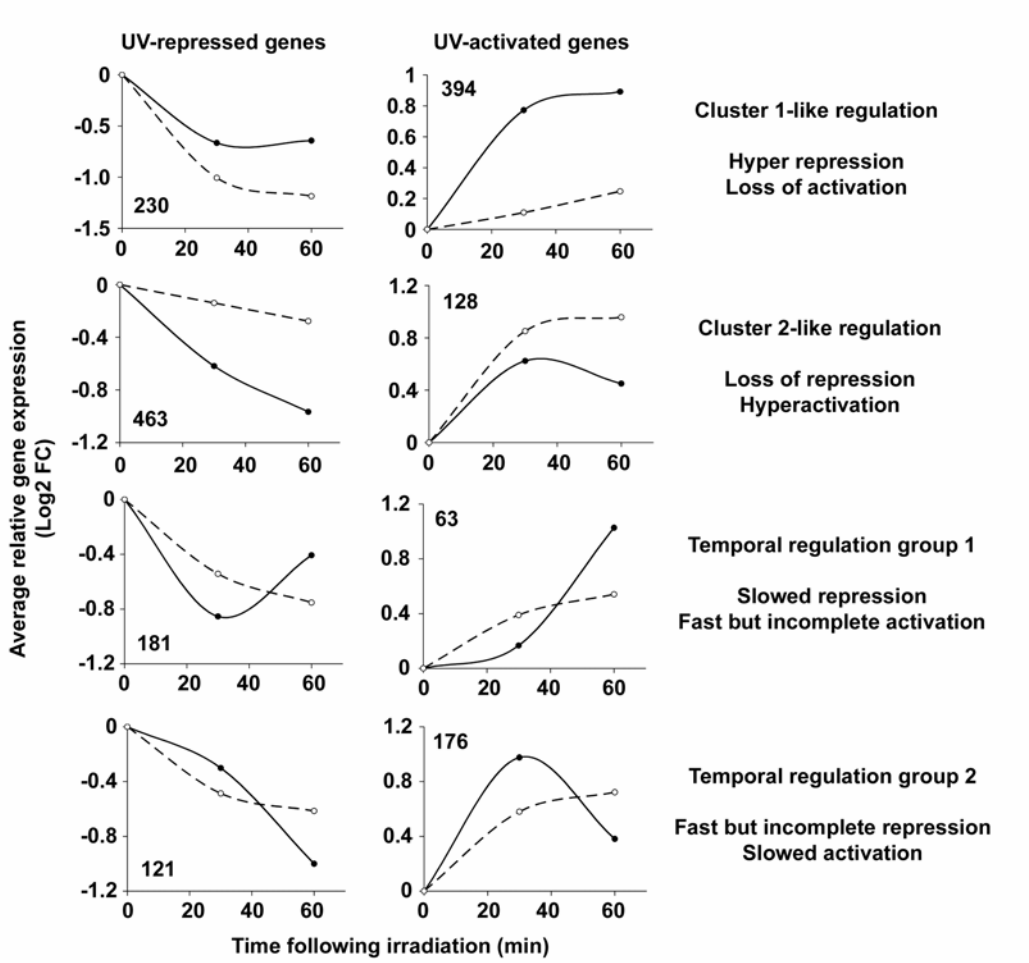

Figure S3: Effects of *rad23*Δ on UV responsive gene expression are similar to loss of Snf1.
Genes in the *rad23Δ* dataset can be grouped into five major clusters. One set of genes were regulated by Rad23 similar to those genes in Snf1 Cluster1, two *rad23*Δ clusters are similar to *snf1*Δ Cluster 2, and two show Rad23-dependent temporal regulation with increased expression early and decreased expression later compared to WT (group 1) or vice versa (group 2). Graphs represent genes in each of these categories separated into UV-activated or UV-repressed subsets. Values are the average gene expression of all genes in a given category at 30 or 60 minutes following irradiation as compared to congenic unirradiated cells. As for *snf1Δ*, many UV-activated and UV-repressed genes have lost full WT UV response in *rad23Δ* cells. In addition, a number of genes displayed improper induction or repression kinetics. One possibility is that these genes were affected differently because of the repair delay in *rad23Δ* cells whereas the Cluster 1- and Cluster 2-like genes are regulated directly by Rad23 even in the absence of damage.

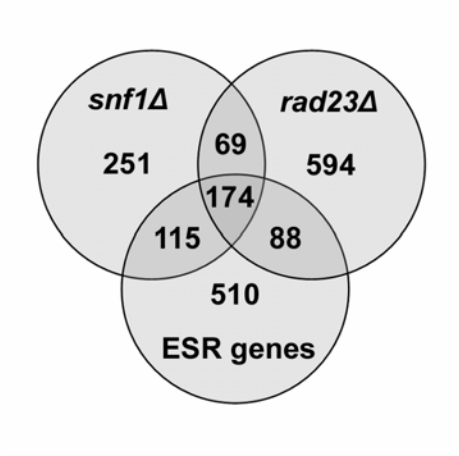

Figure S4: Snf1 and Rad23 regulate 40% of general environmental stress response genes. Gasch et al (2000) identified 887 environmental stress response (ESR) genes whose expression changed in a similar manner across a broad range of stress conditions. The Venn diagram shows the overlap between the ESR set and those genes with significantly different expression in either *snf1Δ* or *rad23Δ* cells compared to WT cells following UV irradiation. About 40% of ESR genes require either Snf1 or Rad23 for proper UV-mediated regulation and about 20% require both factors.

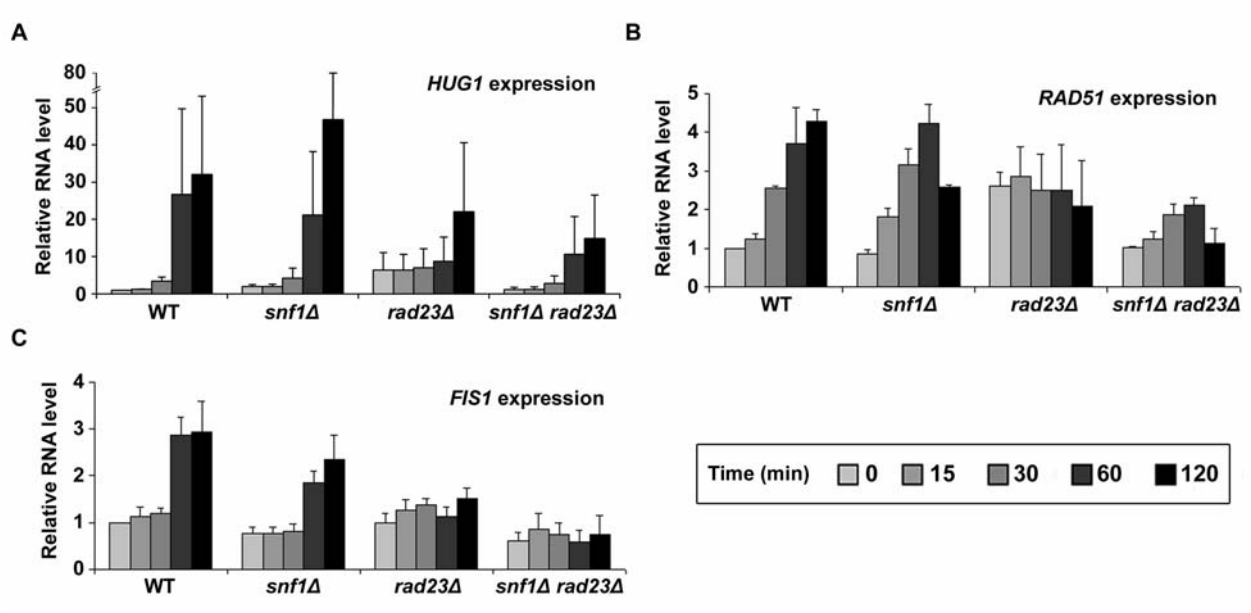

Figure S5: Examples of UV-induced genes that exhibited cooperative regulation by Snf1 and Rad23.

(A-C) Quantitation of Northern blots probed for (A) *HUG1*, (B) *RAD51*, and (C) *FIS1* RNA. Expression of all three genes was induced by UV irradiation with maximum induction at 60 or 120 minutes following damage. Loss of induction was greatest in the *snf1*Δ *rad23*Δ double mutants. This suggests that while both factors are important for proper UV regulation, the presence of one is able to partially compensate for loss of the other (especially in the case of Rad23 compensating for Snf1 loss). Values are the average of three independent experiments and error bars represent standard deviations. Quantitation of the induction level between experiments was variable, particularly for *HUG1*, due to the extremely low uninduced expression levels in WT cells to which all other data was normalized. Nevertheless, the loss of induction seen in mutant cells was consistent across all experiments, as shown in Figures 3E-G.

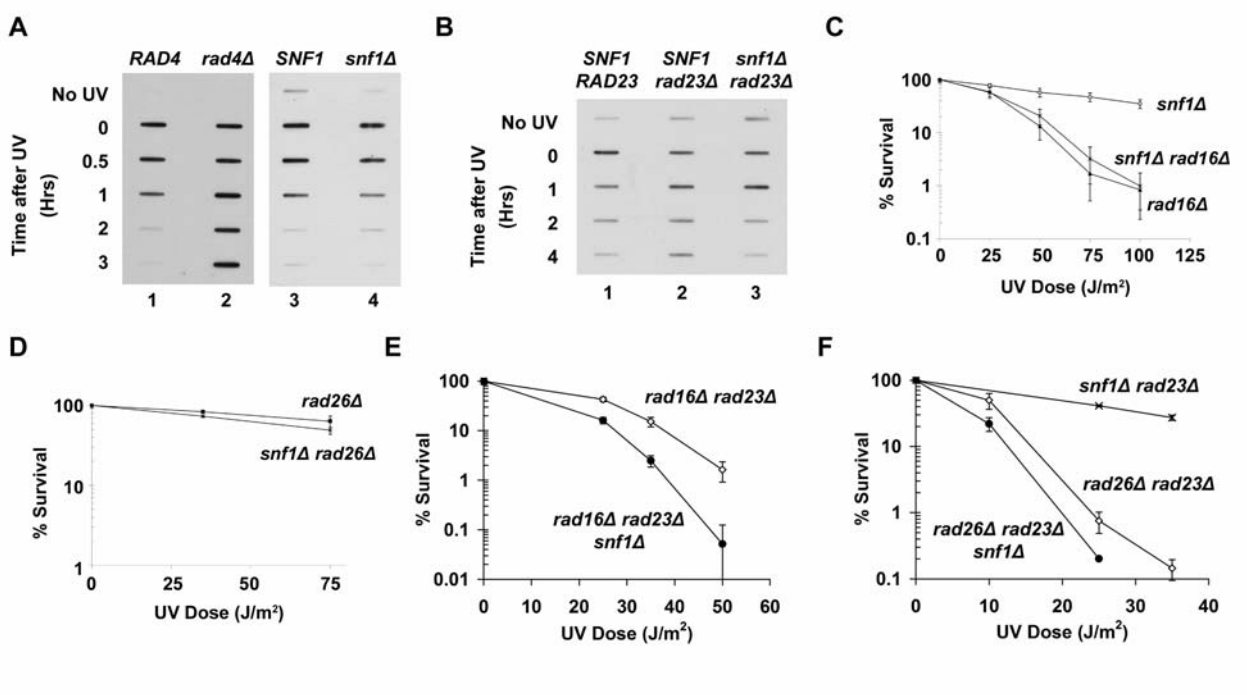

Figure S6: Snf1 is not involved in nucleotide excision repair.

(A-B) Slot blot assay for global removal of cyclobutane pyrimidine dimers (CPDs) from UV irradiated cells. (A), *snf1Δ* cells were as competent in CPD removal as WT cells. (B), The increased UV sensitivity of *snf1Δ rad23Δ* cells could not be explained by diminished repair capacity compared to *rad23Δ* cells. These results did not, however, rule out the possibility that Snf1 is involved in regulation of either transcription coupled NER (TC-NER) or global genomic NER (GG-NER) to an extent not detectable by the slot blot assay. This was addressed by the following genetic analysis.

(C-F) UV survival curves of the indicated strains. Genetic analysis showed no genetic interaction between *SNF1* and either the GG-NER-specific factor, *RAD16,* or the TC-NER-specific factor, *RAD26* (C-D). The increased UV sensitivity imparted by deletion of *SNF1* was still seen in *rad16Δ rad23Δ* and *rad26Δ rad23Δ* cells, placing Snf1 outside of these two NER pathways (E-F). Taken together, these observations strongly suggest that Snf1 is not involved in the repair of UV-induced lesions.

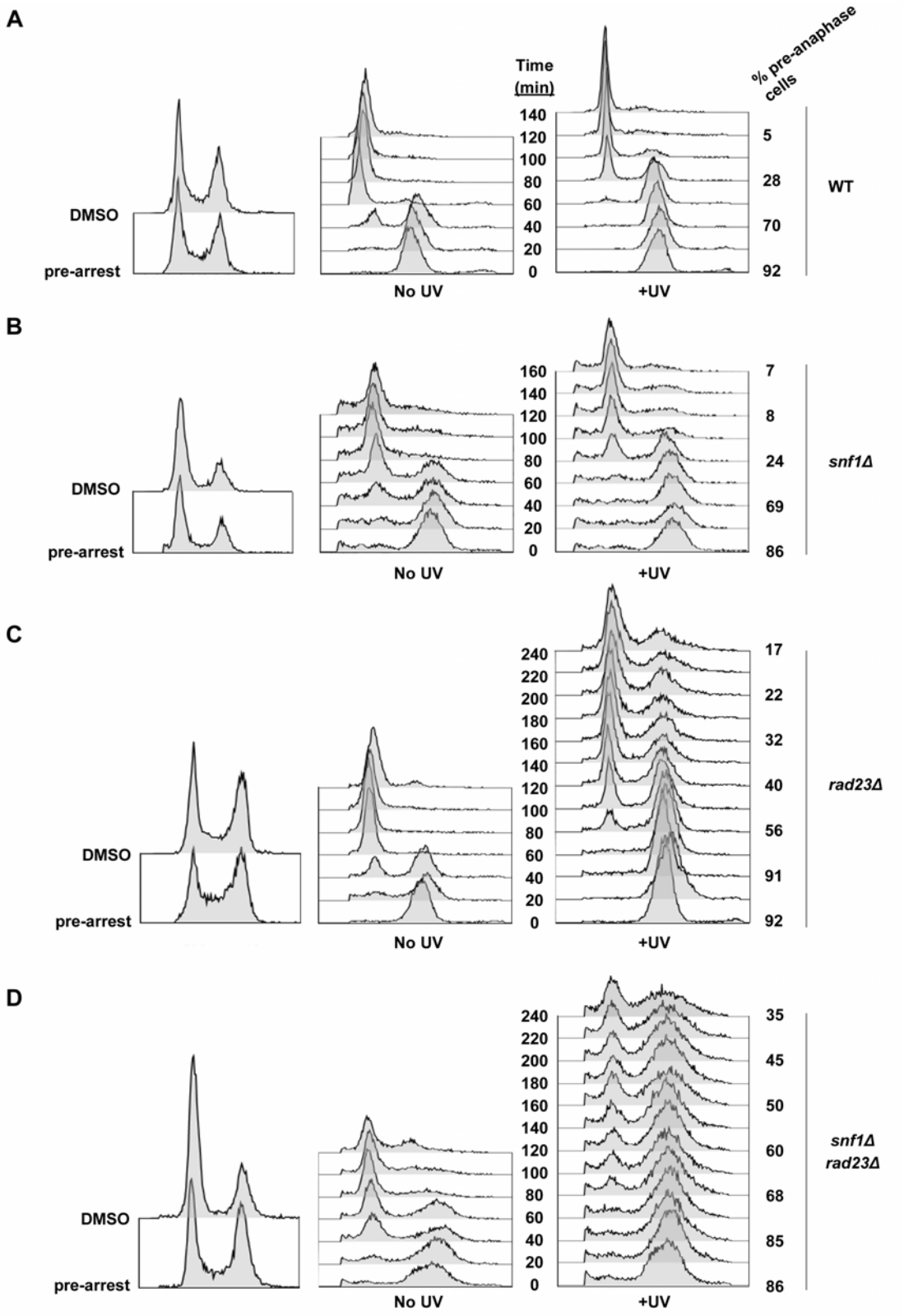
A
B
C
D
DMSO
pre-arrest
No UV
+UV
Time (min)
% pre-anaphase cells
WT
snf1Δ
rad23Δ
snf1Δ rad23Δ

Figure S7: *snf1Δ rad23Δ* cells exhibit delayed recovery from UV-induced G2/M arrest.

(A-D) Flow cytometry of the indicated strains in a *bar1Δ* background. Cells were arrested in G2/M by nocodazole treatment, washed, and released into alpha factor (middle panels, "No UV"). The purpose of the alpha factor addition was to arrest cycling cells in G1 and thereby distinguish the persistently arrested G2 population from cells that had recovered and subsequently passed into a new G2 phase of the cell cycle. Alternatively, cells were arrested in G2/M, washed, and irradiated with 100 J/m^2 UV light prior to release and recovery in alpha factor (right panels, "+UV"). Log-phase pre-arrest cells as well as "DMSO only" (no nocodazole) controls are shown in the far left panels. In addition, irradiated samples were examined by microscopy at 40 minute intervals to determine the percentage of cells that remained arrested in G2/M ("% pre-anaphase cells", shown on the far right). Pre-anaphase cells were defined as large budded cells with single nuclei. Binucleate budded cells which had undergone anaphase or single cells that had cycled into G1 were counted as post-anaphase cells.

(A, B) Wild type and *snf1Δ* cells arrested normally and recovered almost completely by two hours following irradiation.

(C) *rad23Δ* cells arrested for a more extended period, likely due to repair defects. 40% of *rad23*Δ cells remained arrested at two hours, and at four hours 83% had moved past the G2/M arrest.

(D) *snf1Δ rad23Δ* cells arrested following damage, however, these cells had a significant delay in recovery from the arrest compared to *snf1Δ* or *rad23Δ* cells. Four hours following release from nocodazole and irradiation, only 65% of *snf1Δ rad23Δ* cells had moved out of the G2/M arrest. The 35% of cells that were still arrested in G2/M contrasts with the 17% of *rad23Δ* cells that were still arrested at the same time and under the same conditions. This cell cycle delay may contribute to the synthetic UV sensitivity of *snf1Δ rad23Δ* cells.

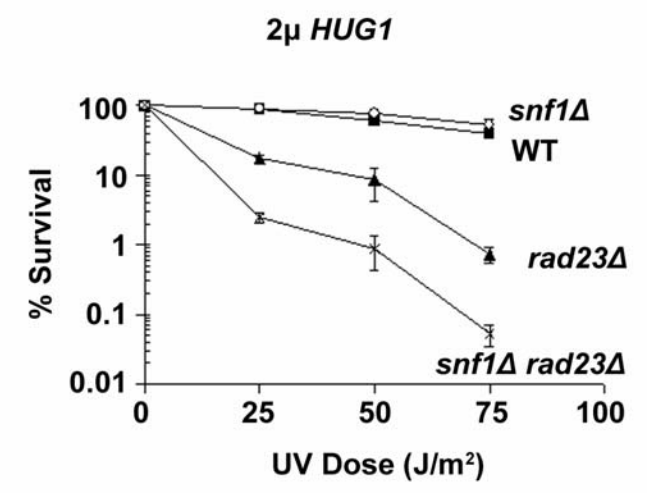

Figure S8: Increased *HUG1* gene dosage did not rescue the UV phenotype of *snf1Δ rad23Δ* cells.

UV survival curve of the indicated yeast strains transformed with a 2µ plasmid carrying the *HUG1* gene. High-copy *HUG1* did not rescue the synthetic UV sensitivity of *snf1Δ rad23Δ* compared to *rad23Δ* cells. These results suggest that loss of *HUG1* induction is not solely responsible for the synthetic phenotype.

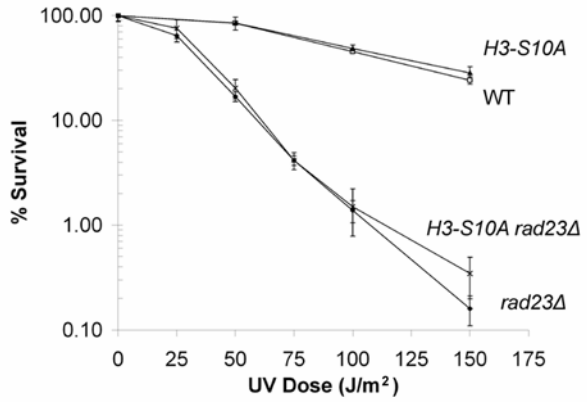

Figure S9: Histone H3-S10 is not important for UV resistance.

UV survival curves of the indicated strains were obtained as in Figure 3A. Error bars represent the standard deviation of the mean for triplicate measurements.

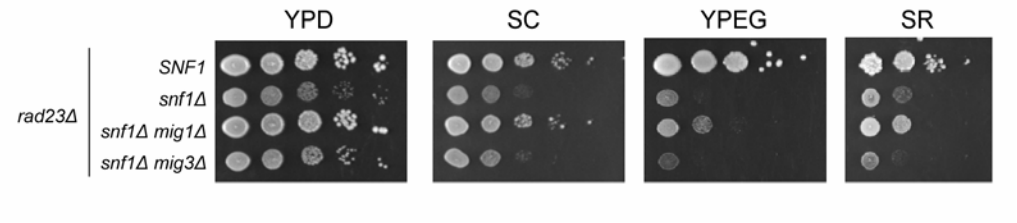

Figure S10: Deletion of *MIG1* but not *MIG3* suppressed the growth defect of *snf1Δ* cells.

10-fold serial dilutions of yeast cultures were spotted onto YPD, synthetic complete media containing 2% glucose (SC), YPEG (2% ethanol, 2% glycerol), and synthetic media containing 2% raffinose (SR). The growth defect of *snf1Δ rad23Δ* cells was the same as that of *snf1Δ* cells (see Figure S1). The slight defect on glucose-containing media was completely suppressed by deletion of *MIG1*. The severe defect on ethanol/glycerol or raffinose-containing media was partially suppressed by *MIG1* deletion. In contrast, no suppression of the *snf1*Δ slow growth phenotype was seen in *snf1*Δ *mig3*Δ cells. These results demonstrate the specificity of *MIG1* for glucose derepression and the starvation response.

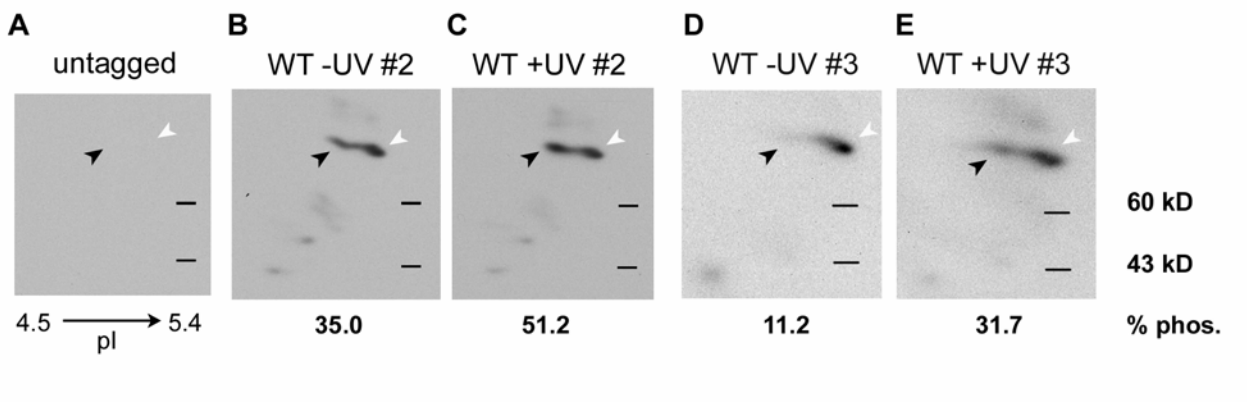

Figure S11: Reproducible increase in Mig3 phosphorylation following UV irradiation.
(A-E) Two-dimensional gel electrophoresis and Western blotting of whole cell extracts for myc-tagged Mig3 prior to (B and D) or 5 minutes following irradiation with 100 J/m^2 UV light (C and E). In (A), extract from untagged cells was analyzed. Although the level of Mig3 phosphorylation was variable in unirradiated cells, a UV-induced 15-20% increase in phosphorylation was highly reproducible.

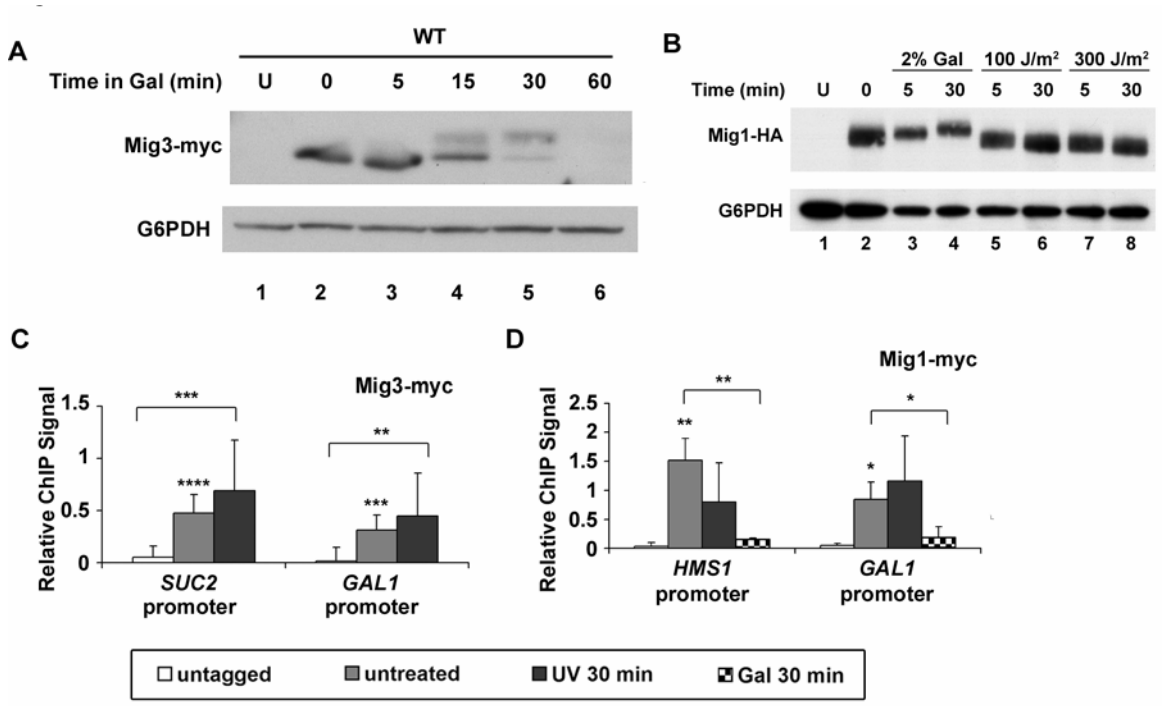

Figure S12: Mig1 and Mig3 are differentially affected by glucose starvation.

(A) Western blot of Mig3-myc following a switch to galactose-containing medium (YEP + 2% galactose). Mig3 was modified ~15 min after the switch and subsequently degraded.

(B) Western blot of Mig1-HA following a switch to 2% galactose-containing media or irradiation with the indicated dose of UV light. Previous results established that Mig1 is phosphorylated following a switch to galactose, a signal which induces Mig1 relocalization to the cytosol (Ahuatzi et al, 2007; De Vit et al, 1997). The shift in Mig1 mobility observed in lanes 3 and 4 versus 2 is consistent with these published results. In contrast, Mig1 was not detectably affected by UV irradiation (lanes 5-8 versus 2). In both (A) and (B), G6PDH was used to control for lane loading and "U" refers to analysis of extract from untagged cells.

(C-D) ChIP data for Mig3-myc (B) and Mig1-myc (C) binding to the indicated promoters. Data were obtained and analyzed as in Figure 6. Mig3 was significantly associated with the Mig1-regulated *SUC2* and *GAL1* promoters and occupancy was unaffected by irradiation. Mig1-myc was released from the *HMS1* and *GAL1* promoters following shift to galactose but not UV treatment. Values are the average of at least three replicates and error bars represent standard deviations. Statistical significance was measured using a two-tailed students t-test with paired variables (**** $p<0.005$, *** $p<0.01$, ** $p<0.03$, * $p<0.05$).

Figure S13: Rad4 regulates transcription of very few genes compared to Rad23.
Venn diagram showing genes that were significantly affected by *rad23*Δ or *rad4*Δ (FDR cutoff 5%). Expression of only 237 genes was affected by deletion of *RAD4*, relatively few compared to the more than 2200 that were Rad23-dependent. The overlap between these two data sets was not significant. The overlap actually represents fewer genes regulated by both Rad23 and Rad4 than would be expected by chance ($p = 0.042$). Therefore, Rad23 does not regulate transcription in the context of the Rad23-Rad4 complex.

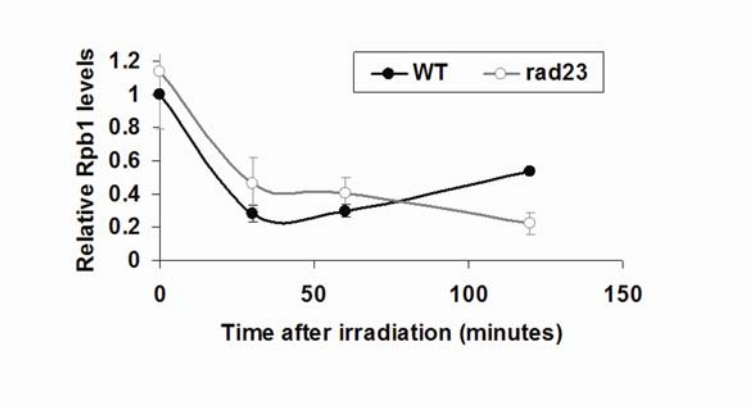

Figure S14: Rad23 did not affect UV-induced Rpb1 degradation.
Quantitation of western blots of whole cell extracts from UV-irradiated WT or *rad23Δ* cells showed that *rad23Δ* cells were able to degrade the RNA polymerase II subunit Rpb1 properly following damage. There was some lag in recovery of Rpb1 levels that may be attributable to the fact that *rad23*Δ cells retained UV-induced lesions longer (Figure S6). However, this difference at two hours post-irradiation cannot explain differences in transcription observed at 30 and 60 minutes following irradiation. Three independent experiments were performed and error bars represent the standard deviation. Protein levels were normalized to G6PDH levels.

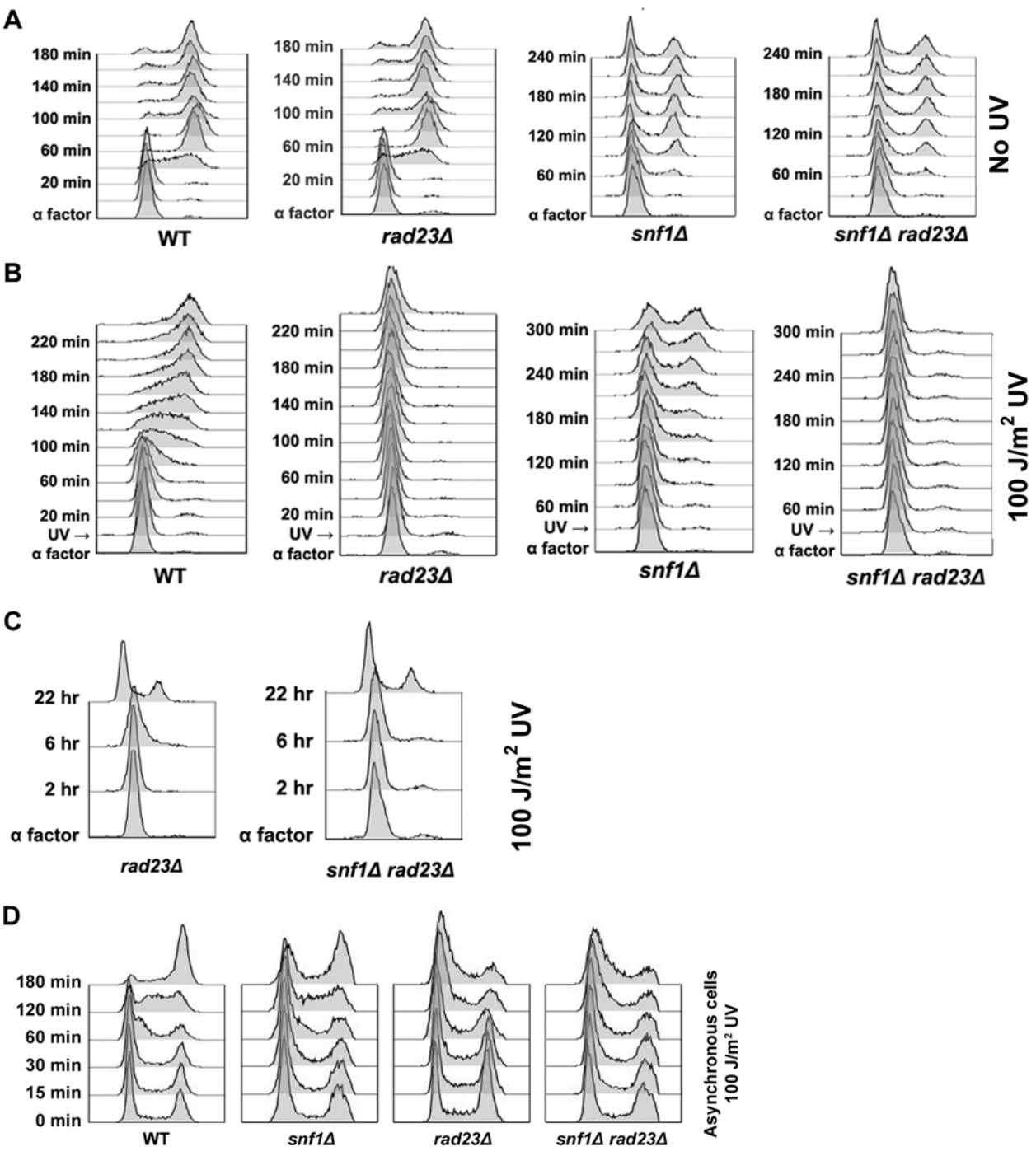
A
180 min
140 min
100 min
60 min
20 min
α factor
WT
180 min
140 min
100 min
60 min
20 min
α factor
rad23Δ
240 min
180 min
120 min
60 min
α factor
snf1Δ
240 min
180 min
120 min
60 min
α factor
snf1Δ rad23Δ
No UV
B
220 min
180 min
140 min
100 min
60 min
20 min
UV →
α factor
WT
220 min
180 min
140 min
100 min
60 min
20 min
UV →
α factor
rad23Δ
300 min
240 min
180 min
120 min
60 min
UV →
α factor
snf1Δ
300 min
240 min
180 min
120 min
60 min
UV →
α factor
snf1Δ rad23Δ
100 J/m2 UV
C
22 hr
6 hr
2 hr
α factor
rad23Δ
22 hr
6 hr
2 hr
α factor
snf1Δ rad23Δ
100 J/m2 UV
D
180 min
120 min
60 min
30 min
15 min
0 min
WT
snf1Δ
rad23Δ
snf1Δ rad23Δ
Asynchronous cells
100 J/m2 UV

Figure S15: *snf1Δ rad23Δ* cells do not have a cell cycle arrest defect.

(A-C) Flow cytometry of the indicated strains in a *bar1Δ* background. Cells were arrested in G1 by alpha factor treatment, washed and allowed to recover from arrest over the indicated time course (A, unirradiated controls). Alternatively, cells were arrested in G1, washed and UV irradiated prior to recovery to assess the UV-induced arrest over the indicated time course (B and C). Wild type cells arrested normally and began to recover following repair at about 80 minutes (B, first panel). *rad23Δ* cells arrested for an extended period because they were unable to completely repair the damage within the 4 hour time course (B, second panel). *snf1Δ rad23Δ* cells properly arrested following damage while repair was occurring (B, fourth panel). This suggests that the phenotype seen in these cells was not due to replication of damaged DNA. *snf1Δ* cells did not properly recover from alpha factor arrest even in the absence of UV irradiation. Both *rad23Δ* and *snf1Δ rad23Δ* cells eventually recovered from the extended arrest (C).

(D) Flow cytometry of asynchronous cells from indicated strains in a *BAR1* background. Results are consistent to those seen with G1 synchronized cells. WT cells arrested following irradiation and released from the cell cycle checkpoint following repair with most G1-arrested cells moving into S phase by two hours. Although *snf1Δ* cells were slower to cycle, they had a profile similar to WT cells prior to and within the first hour of UV-induced arrest. As expected, both *rad23Δ* and *snf1Δ rad23Δ* cells remained arrested throughout a three hour time course. All four strains had a very similar cell cycle profile during the arrested period (within one hour of irradiation). This argues against differences in cell cycle distribution as a cause of the observed transcriptional changes.

SUPPLEMENTARY TABLES

Table S1: Significantly UV-regulated genes

See attached excel spreadsheet for microarray data of genes with significant changes in gene expression within one hour of UV irradiation in WT cells.

Table S2: GO term analysis of UV regulated genes

UV treatment	Regulation	Over-represented GO terms (Process)	# of genes/ genes affected	p-value
WT UV treated – 15 min	Activated	Cell cycle	25/139	$1.7x10^{-5}$
	Repressed	Cell cycle	16/58	$3.6x10^{-6}$
WT UV treated – 30 min	Activated	Nitrogen compound metabolic process	46/521	$2.8x10^{-7}$
		Amino acid metabolism	37	$1.9x10^{-7}$
		Carboxylic acid metabolism	49	$1.8x10^{-4}$
		Sulfur metabolism	18	$1.5x10^{-3}$
		Vitamin transport	6	$7.1x10^{-3}$
	Repressed	Establishment and maintenance of chromatin structure	48/511	$9.9x10^{-8}$
		Chromatin modification	38	$1.3x10^{-4}$
		Chromatin assembly/disassembly	27	$3.1x10^{-5}$
		Chromatin remodeling	28	$1.3x10^{-3}$
		Regulation of gene expression	67	$2.1x10^{-6}$
		Cell cycle	59	$4.2x10^{-6}$
		Regulation of cell cycle	30	$3.8x10^{-4}$
		Chromosome segregation	25	$7.8x10^{-4}$
		Response to stimulus	97	$8.4x10^{-6}$
		Response to stress	66	$1.4x10^{-4}$
		DNA repair	32	$2.8x10^{-3}$
		Signal transduction	38	$2.9x10^{-5}$
WT UV treated – 60 min	Activated	Response to stimulus	93/495	$1.3x10^{-5}$
		Response to stress	68	$3.7x10^{-6}$
		Response to oxidative stress	19	$1.9x10^{-4}$
		Catabolic process	58	$4.2x10^{-4}$
		Heteroduplex formation	6	$4.4x10^{-3}$
	Repressed	Organelle organization and biogenesis	291/791	$6.1x10^{-30}$
		Ribosome biogenesis and assembly	138	$2.6x10^{-35}$
		RNA metabolic process	168	$2.1x10^{-18}$
		rRNA metabolic process	79	$2.9x10^{-16}$
		tRNA metabolic process	34	$9.5x10^{-5}$
		Gene expression	217	$1.0x10^{-8}$
		Regulation of gene expression	91	$9.9x10^{-7}$
		Establishment and maintenance of chromatin structure	59	$3.2x10^{-6}$
		Chromatin remodeling	41	$8.8x10^{-6}$
		Chromatin assembly/disassembly	34	$4.9x10^{-5}$
		Chromatin modification	49	$3.4x10^{-4}$
		Cell cycle	71	$1.8x10^{-3}$

Table S3: GO term analysis of Rad23- and Snf1-regulated genes

Factor	Regulation	Over-represented GO terms (Process)	# of genes/ genes affected	p-value
Snf1	Activated	Organelle organization and biogenesis	412/1037	$1.8x10^{-54}$
		Ribosome biogenesis and assembly	189	$5.1x10^{-55}$
		Nucleic acid metabolic process	355	$2.7x10^{-47}$
		RNA metabolic process	266	$1.7x10^{-48}$
		rRNA metabolic process	111	$1.3x10^{-27}$
		tRNA metabolic process	49	$1.8x10^{-9}$
		Gene expression	315	$9.2x10^{-21}$
		Regulation of gene expression	110	$4.3x10^{-6}$
		Gene silencing	36	$2.0x10^{-5}$
		Cell cycle	108	$3.1x10^{-10}$
		DNA replication	47	$3.0x10^{-8}$
		Sister chromatid cohesion	19	$2.1x10^{-6}$
		Regulation of cell cycle	48	$1.5x10^{-4}$
		Nuclear transport	48	$1.5x10^{-8}$
		Protein transport	70	$4.9x10^{-5}$
		Chromosome organization and biogenesis	135	$9.5x10^{-7}$
		Chromatin remodeling	53	$7.8x10^{-8}$
		Chromatin modification	63	$1.8x10^{-5}$
		Intracellular protein transport	69	$1.7x10^{-5}$
		Protein targeting	63	$9.6x10^{-5}$
	Repressed	Generation of precursor metabolites/energy	62/1076	$1.9x10^{-10}$
		Oxidative phosphorylation	34	$2.7x10^{-15}$
		ATP metabolic process	16	$1.3x10^{-7}$
		Ion transport	49	$9.9x10^{-10}$
		Proton transport	17	$8.7x10^{-7}$
		Phosphate metabolic process	72	$2.0x10^{-9}$
		Cell wall organization and biogenesis	67	$1.0x10^{-7}$
		Carbohydrate metabolic process	60	$2.7x10^{-7}$
		Response to stimuli	168	$9.6x10^{-5}$
		Response to chemical stimulus	106	$7.2x10^{-7}$
		Response to oxidative stress	27	$3.2x10^{-3}$
		Vitamin metabolic process	38	$1.2x10^{-6}$
		Nucleotide metabolic process	37	$1.5x10^{-4}$
		Sulfur metabolic process	28	$3.3x10^{-4}$
Rad23	Activated	Organelle organization and biogenesis	431/1142	$5.5x10^{-50}$
		Ribosome biogenesis and assembly	143	$7.7x10^{-20}$
		Nucleic acid metabolic process	352	$6.4x10^{-35}$
		RNA metabolic process	281	$6.9x10^{-48}$
		rRNA metabolic process	91	$2.5x10^{-12}$
		mRNA metabolic process	73	$1.2x10^{-8}$
		Establishment and maintenance of chromatin structure	106	$2.6x10^{-21}$
		Chromatin modification	89	$3.4x10^{-16}$
		Chromatin remodeling	69	$1.4x10^{-15}$
		Chromatin assembly/disassembly	48	$9.1x10^{-8}$
		Intracellular transport	176	$9.6x10^{-21}$
		Nuclear transport	52	$2.5x10^{-9}$
		Vesicle-mediated transport	98	$4.0x10^{-8}$
		Protein transport	80	$5.6x10^{-7}$
		Nucleic acid transport	35	$1.1x10^{-6}$
		Gene expression	330	$6.6x10^{-18}$

Factor	Regulation	Over-represented GO terms (Process)	# of genes/ genes affected	p-value
		Transcription	94	$2.4x10^{-16}$
		Regulation of gene expression	122	$2.7x10^{-7}$
		Gene silencing	35	$8.1x10^{-4}$
	Repressed	Generation of precursor metabolites/energy	74/1105	$2.5x10^{-17}$
		Oxidative phosphorylation	34	$6.9x10^{-15}$
		ATP metabolic process	16	$2.1x10^{-7}$
		Transport	199	$1.1x10^{-3}$
		Ion transport	51	$1.6x10^{-10}$
		Proton transport	18	$9.9x10^{-8}$
		Amino acid transport	20	$4.4x10^{-4}$
		Carboxylic acid transport	25	$6.1x10^{-5}$
		Carbohydrate metabolic process	65	$3.1x10^{-9}$
		Alcohol metabolic process	57	$1.3x10^{-7}$
		Phosphate metabolic process	68	$5.5x10^{-7}$
		Vitamin metabolic process	36	$4.0x10^{-5}$
		Response to chemical stimulus	98	$9.1x10^{-4}$
		Sporulation	40	$2.4x10^{-3}$
		Nucleotide metabolic process	35	$5.9x10^{-3}$

Table S4: Statistical analysis of overlap with *rad23Δ* microarray data sets.

rad23 vs…	*snf1Δ*		*rpn11-[D1223]*		*rpt1S*		*pre1-1*	
Case	No. of genes	p-value	No. of genes	p-value	No. of genes	p-value	No. of genes	p-value
U U	2050	0.0006	1849	0.0003	2518	0.0004	2165	0.2447
U A	892	<0.0001	927	<0.0001	258	<0.0001	611	0.2742
A U	1026	<0.0001	1302	<0.0001	1854	<0.0001	1678	0.2742
A A	1221	0.0006	827	0.0003	275	0.0004	451	0.2447
Analysis taking into account direction of regulation…								
- -	501	0.0008	310	0.0003	131	0.0009	89	<0.0001
- U	614	<0.0001	725	0.07	957	0.017	910	0.0003
- +	27	<0.0001	59	<0.0001	6	<0.0001	95	0.0083
U -	491	<0.0001	537	0.1447	194	0.0045	305	0.4669
U U	2050	0.0008	1849	0.0003	2518	0.0009	2165	0.2558
U +	401	<0.0001	390	<0.0001	64	0.0017	306	0.2642
+ -	45	<0.0001	130	<0.0001	59	0.0036	142	0.0025
+ U	412	<0.0001	577	<0.0001	897	0.0054	768	<0.0001
+ +	648	0.0008	328	0.0003	79	0.0009	125	0.052

U = unaffected, A = affected in mutant , - = down-regulated in mutant, + = up-regulated in mutant
black = enrichment, red = depletion

The analysis method is described in Supplementary Materials and Methods. Upper rows show statistical significance of enrichment (black) where the actual overlap exceeds the random overlap or depletion (red) where the actual overlap falls below the random overlap within the datasets of every possible comparison between *rad23Δ* and *snf1Δ* or the individual proteasome mutants. Cases are defined by "U", unaffected, and "A", affected, with the first value corresponding to the *rad23Δ* dataset and the second value to *snf1Δ* or the proteasome mutant. Overall, when comparing the *rad23Δ* data to either *rpn11*, *rpt1* or *snf1Δ* datasets, this analysis reveals cases of significantly enrichment for genes that were affected or unaffected in both mutants (low p-value in black for the AA and UU cases). Alternatively, instances of significant depletion for genes regulated by only one of the two factors were also uncovered (low p-values in red for the UA and AU cases). In the case of Pre1, high p-values were calculated in all cases. The nine lower rows indicate statistical significance of enrichment (black) or depletion (red) within the datasets of each possible relationship between *rad23Δ* and *snf1Δ* or the individual proteasome mutants taking into account the direction of regulation. Cases are defined by "–", down-regulated, "U", unaffected, "+", up-regulated, with the first value corresponding to the *rad23Δ* dataset and the second value to *snf1Δ* or the proteasome mutant. Overall, for comparison of *rad23Δ* with *rpn11*, *rpt1*, or *snf1Δ* the datasets are enriched in genes that are activated or repressed in both mutants (low p-values in black for the - - and + + cases) and depleted for genes that are discordantly regulated by the two factors (low p-value in red for the - + or + - cases).

Table S5: Gene expression data for all genes studied in ChIP experiments.

	HUG1 expression			*HMS1* expression			*SUC2* expression			*GAL1* expression			*ACT1* expression		
Strain	YPD* No UV	UV**	Gal***	YPD No UV	UV	Gal	YPD No UV	UV	Gal	YPD No UV	UV	Gal	YPD No UV	UV	Gal
WT	1.0	27 ±23	1.2 ±0.6	1.0	0.3 ±0.1	3.3 ±0.8	1.0	1.1 ±0.3	26 ±5.7	1.0	0.9 ±0.6	4.4 ±3.0	1.0	1.4 ±0.3	0.6 ±0.1
snf1Δ	2.7 ±1.6	21 ±17	3.0 ±1.1	1.4 ±0.3	0.2 ±0.03	4.6 ±0.9	0.9 ±0.5	1.0 ±0.1	0.4 ±0.1	1.8 ±1.6	1.1 ±0.3	1.1 ±0.4	0.8 ±0.2	0.9 ±0.2	0.6 ±0.1
rad23Δ	6.5 ±4.8	8.7 ±6.4	4.0 ±3.2	1.6 ±0.8	0.4 ±0.04	1.6 ±0.6	4.0 ±2.6	2.3 ±0.6	42 ±14	1.2 ±0.4	1.7 ±0.2	1.1 ±0.3	0.8 ±0.1	0.6 ±0.1	0.6 ±0.2
snf1Δ rad23Δ	1.8 ±1.1	11 ±10	1.6 ±0.1	1.1 ±0.3	0.3 ±0.1	4.0 ±1.3	1.0 ±0.1	1.0 ±0.3	0.8 ±0.1	1.3 ±1.0	3.1 ±1.0	1.2 ±0.3	0.8 ±0.2	0.9 ±0.2	0.4 ±0.1
mig1Δ	6.0 ±3.5	ND	6.1 ±2.7	1.0 ±0.1	ND	2.6 ±1.1	5.0 ±1.6	ND	73 ±50	0.8 ±0.1	ND	19 ±25	1.3 ±0.5	ND	0.8 ±0.4
mig3Δ	17 ±5.9	18 ±11	9.3 ±5.3	0.5 ±0.1	0.3 ±0.1	2.7 ±0.7	1.1 ±0.4	1.3 ±0.7	59 ±21	0.6 ±0.2	0.6 ±0.2	0.9 ±0.1	1.3 ±0.3	1.6 ±0.6	0.9 ±0.1

* Expression values from log phase yeast growing in YPD prior to irradiation.

** Expression values 60 minutes following irradiation with 100 J/m^2 UV light.

*** Expression values 60 minutes after switching log phase cells from YPD (2% glucose) to YPG (2% galactose).

TABLE S6: Yeast strains used in this study.

Strain	Genotype	Reference or Source
YPH499	*MATa ura3-52 lys3-52 lys2-801a ade2-101a trp1-Δ63 his3-Δ200 leu2-Δ1*	Sikorski & Hieter
YPH500	*MATα ura3-52 lys3-52 lys2-801a ade2-101a trp1-Δ63 his3-Δ200 leu2-Δ1*	Sikorski & Hieter
JJSY664	*MATa * snf1Δ::KAN*	This study
JJSY661	*MATa *rad23Δ::HIS3*	This study
SLW116	*MATa * snf1Δ::KAN rad23Δ::HIS3*	This study
SLW101	*MATa his3Δ1 leu2Δ met15Δ ura3Δ snf4Δ::NAT*	This study
SLW102	*MATa his3Δ1 leu2Δ met15Δ ura3Δ snf4Δ::NAT rad23Δ::KAN*	This study
JJSY778	*MATα * rad4Δ::KAN*	This study
AY68	*MATα * rad16Δ::URA3*	Ramsey et.al.
SLW237	*MATa * snf1Δ::KAN rad16Δ::URA3*	This study
SLW235	*MATa * rad23Δ::HIS3 rad16Δ::URA3*	This study
SLW239	*MATa * snf1Δ::KAN rad23Δ::HIS3 rad16Δ::URA3*	This study
SLW253	*MATα * rad26Δ::NAT*	This study
SLW257	*MATa * snf1Δ::KAN rad26Δ::NAT*	This study
SLW255	*MATa * rad23Δ::HIS3 rad26Δ::NAT*	This study
SLW259	*MATa * snf1Δ::KAN rad26Δ::NAT rad23Δ::HIS3*	This study
MSY1843	*MATa his3d1 leu2d ura3d0 hht1-hhf1::KAN hht2-hhf2d::NAT hta1-htb1d::HPH hta2-htb2::NAT pQQ18[HTA1 HTB1 HHF2 HHT2 LEU2 CEN]*	M. Smith
MSY1843-H3S10A	*MATa his3d1 leu2d ura3d0 hht1-hhf1::KAN hht2-hhf2d::NAT hta1-htb1d::HPH hta2-htb2::NAT pQQ18-H3S10A[HTA1 HTB1 HHF2 hht2-S10A LEU2 CEN]*	M. Smith
SLW185	*MATa his3d1 leu2d ura3d0 hht1-hhf1::KAN hht2-hhf2d::NAT hta1-htb1d::HPH hta2-htb2::NAT rad23Δ::HIS3 pQQ18[HTA1 HTB1 HHF2 HHT2 LEU2 CEN]*	This study
SLW186	*MATa his3d1 leu2d ura3d0 hht1-hhf1::KAN hht2-hhf2d::NAT hta1-htb1d::HPH hta2-htb2::NAT rad23Δ::HIS3 pQQ18-H3S10A[HTA1 HTB1 HHF2 hht2-S10A LEU2 CEN]*	This study
SLW204	*MATα * mig1Δ::NAT*	This study
SLW205	*MATα * mig3Δ::NAT*	This study
SLW209	*MATa * mig1Δ::NAT rad23Δ::HIS3*	This study
SLW216	*MATa * rad23Δ::HIS3*	This study
SLW220	*MATα * mig3Δ::NAT rad23Δ::HIS3*	This study
SLW225	*MATa * snf1Δ::KAN mig1Δ::NAT*	This study
SLW227	*MATa * snf1Δ::KAN rad23Δ::HIS3 mig1Δ::NAT*	This study
SLW221	*MATa * snf1Δ::KAN mig3Δ::NAT*	This study
SLW223	*MATa * snf1Δ::KAN rad23Δ::HIS3 mig3Δ::NAT*	This study
SLW111	*MATa * snf1Δ::KAN rad23Δ::HIS3 pSNF1-316[SNF1 URA3 CEN] pRAD23-315[RAD23 LEU2 CEN]*	This study
SLW152	*MATa * snf1Δ::KAN rad23Δ::HIS3 pK84R-315[snf1-K84R LEU2 CEN] pRS316[URA3 CEN]*	This study
SLW154	*MATa * snf1Δ::KAN rad23Δ::HIS3 pRS315[LEU2 CEN] pRS316[URA3 CEN]*	This study
SLW318	*MATa * snf1Δ::KAN rad23Δ::HIS3 pSNF1-316[SNF1 URA3 CEN]*	This study

SLW319	*MATa * snf1Δ::KAN rad23Δ::HIS3 pT210A-316 [snf1-T210A URA3 CEN]*	This study
SLW320	*MATa * snf1Δ::KAN rad23Δ::HIS3 pRS316 [URA3 CEN]*	This study
SLW188	*MATa * snf1Δ::KAN pSNF1-315 [LEU2 CEN]*	This study
SLW189	*MATa * snf1Δ::KAN pSNF1HA-315 [SNF1-HA LEU2 CEN]*	This study
SLW342	*MATa * elm1Δ::NAT sak1Δ::NAT tos3Δ::KAN*	This study
SLW343	*MATa * elm1Δ::NAT sak1Δ::NAT tos3Δ::KAN rad23Δ::HIS3*	This study
SLW300	*MATa * MIG3MYC-TRP1*	This study
SLW302	*MATa * MIG3MYC-TRP1 snf1Δ::KAN*	This study
SLW368	*MATa * MIG3MYC-TRP1 rad23Δ::HIS*	This study
SLW377	*MATa * MIG1MYC-TRP*	This study
SLW361	*MATa * rad23Δ::HIS3 pRAD23-315[RAD23 LEU2 CEN]*	This study
SLW362	*MATa * rad23Δ::HIS3 prad23Δubl-315[rad23ΔUbL LEU2 CEN]*	This study
SLW363	*MATa * rad23Δ::HIS3 pRS315[LEU2 CEN]*	This study
YJR535	*MATa * sml1Δ::URA3*	J. Reese
YJR748	*MATa * mec1Δ::LEU2 tel1Δ::KAN sml1Δ::URA3*	J. Reese
SLW337	*MATa * sml1Δ::URA3 pSNF1HA-314[SNF1HA TRP1 CEN]*	This study
SLW338	*MATa * pSNF1-315[SNF1 LEU2 CEN]*	This study
SLW340	*MATa * pSNF1HA-315[SNF1HA LEU2 CEN]*	This study
SLW341	*MATa * mec1Δ::LEU2 tel1Δ::KAN sml1Δ::URA3 pSNF1HA-314[SNF1HA TRP1 CEN]*	This study
SLW345	*MATa * bar1Δ::NAT*	This study
SLW344	*MATa * rad23Δ::HIS3 bar1Δ::NAT*	This study
SLW349	*MATa * bar1Δ::NAT snf1Δ::KAN*	This study
SLW351	*MATa * bar1Δ:NAT snf1Δ:KAN rad23Δ:HIS3*	This study

** ura3-52 lys3-52 lys2-801a ade2-101a trp1-Δ63 his3-Δ200 leu2-Δ1*

TABLE S7: Plasmids used in this study.

Plasmid	Characteristics	Source
pSNF1-315	*SNF1 LEU CEN*	This study
pSNF1-316	*SNF1 URA CEN*	This study
pK84R-315	*snf1-K84R LEU2 CEN*	This study
pSNF1HA-315	*SNF1-3HA LEU2 CEN*	M. Schmidt
pSNF1HA-314	*SNF1-3HA TRP1 CEN*	This study
pT210A-316	*snf1-T210A-3HA URA3 CEN*	M. Schmidt
pRAD23-315	*RAD23 LEU2 CEN*	This study
prad23ΔUbL-315	*rad23ΔUbL LEU2 CEN*	This study
pQQ18	*HTA1 HTB1 HHF2 HHT2 LEU2 CEN*	M. Smith
pQQ18-H3S10A	*HTA1 HTB1 HHF2 hht2-S10A LEU2 CEN*	M. Smith

SUPPLEMENTARY MATERIALS AND METHODS

Comparison of *rad23Δ* and proteasome mutant microarray data: As described in the Materials and Methods section, genes were classified as differentially regulated at a 5% FDR. In the top of Table S4, we denote affected genes by "A" and unaffected genes by "U" for both our *rad23Δ* versus wild type differential expression data and the proteasome mutant differential expression data (Auld et al. 2006). In the bottom of Table S4, we denote up-regulated genes by "+", down-regulated genes by "–" and unaffected genes by "U". The significance of the number of matches between the *rad23Δ* and proteasome mutant differential expression calls (i.e., "U", "A", "+", or "–") was tested by randomly permuting the proteasome calls relative to the *rad23Δ* calls 10,000 times. The enriched p-values were estimated by calculating the fraction of random matches that exceeded the actual number of matches for each case. Similarly, the depleted p-values were estimated by calculating the fraction of random matches that were less than the actual number of matches for each case.

GO term analysis of microarray data: Lists of significantly affected genes for UV irradiated and mutant samples were analyzed for significant enrichment of gene ontology (GO) terms using the Gene Ontology Term Finder at the Sacchromyces Genome Database (www.yeastgenome.org).

Slot blot: Cells were grown in YPD to an OD600 of 1.0, resuspended in water, treated with 60 or 100 J/m^2 UV irradiation, and returned to YPD. Samples were taken prior to UV irradiation and at the indicated time points following treatment. For each sample 500 ng of genomic DNA was incubated at 65ºC for 30 minutes in 0.1M NaOH. An equal volume of cold 2M sodium acetate pH 7.0 was added and samples were applied to a nylon membrane using a slot blot apparatus (Hoefer) according to the manufacturer's instructions. Slots were washed with 2 X SSC and the membrane was baked at 80ºC for 2 hours. Membranes were blocked overnight at 4ºC in TBST containing 0.5% milk. Primary CPD antibody (Kamiya Biomedical) was applied at 1:250 dilution in 0.5X TBST. Washing, secondary antibody incubation, and visualization were done as described in the main Materials and Methods section.

Flow cytometry: All flow cytometry experiments were performed using *bar1*Δ strains. For nocodazole synchronization experiments in Figure S7, cells were grown at 30ºC in YPD to an OD600 of 0.5 and arrested with 15 μg/ml nocodazole for 3 hours (WT and *rad23*Δ cells) or 6

hours (*snf1*Δ and *snf1*Δ *rad23*Δ cells). Following arrest, cells were washed three times in pre-warmed sterile water. During the last wash, half of the cells were irradiated with 100 J/m^2 UV light and returned to pre-warmed YPD media containing 50 nM alpha-factor. Unirradiated cells were also resuspended in fresh pre-warmed YPD containing alpha-factor. For alpha factor arrest experiments in Figure S15, cells were grown as described above and arrested with the mating pheromone alpha-factor as described in Yellman and Burke (2004). Following arrest, cells were washed three times in prewarmed sterile water. During the last wash, half of the cells were irradiated with 100 J/m^2 UV light and returned to prewarmed YPD media. Unirradiated cells were also resuspended in fresh prewarmed YPD. For both experiments, samples were taken at the indicated time point, fixed and prepared for flow cytometry as described in Yellman and Burke (2004). Briefly, cells were fixed in 70% ethanol, RNase treated, pepsin treated and stained for DNA with Sytox green (Invitrogen). Cells were sonicated prior to flow cytometry, which was performed at the UVA Flow Cytometry Core Facility using a Becton Dickinson FACSCalibur dual laser benchtop cytometer. In addition, cells were visualized by fluorescence microscopy and manually counted for the number of cells in G2/M (budding cells with single nuclei) or post-anaphase (binucleate budding cells or single cells in G1).

Western blotting: Rpb1 western blotting was done using the 8WG16 monoclonal antibody from Covance at a dilution of 1:500.

Two-dimensional gel electrophoresis: Two-dimensional electrophoresis was performed according to the carrier ampholine method of isoelectric focusing (O'Farrell, 1975) by Kendrick Labs, Inc. (Madison, WI) as follows: Isoelectric focusing was carried out in a glass tube of inner diameter 2.0 mm using 1% pH 4-6 and 1% pH 5-8 ampholines (GE Healthcare) for 9600 volt-hrs. The tube gel pH gradient was determined with a surface pH electrode. After equilibration for 10 min in Buffer O (10% glycerol, 50 mM dithiothreitol, 2.3% SDS and 0.0625 M Tris, pH 6.8), each tube gel was sealed to the top of a stacking gel that overlaid a 10% acrylamide slab gel (0.75 mm thick). SDS slab gel electrophoresis was carried out for about 4 hours at 15 mA per gel. After electrophoresis, the gel was transblotted onto PVDF overnight at 200 mA.

SUPPLEMENTARY REFERENCES

Ahuatzi D, Riera A, Pelaez R, Herrero P, Moreno F (2007) Hxk2 regulates the phosphorylation state of Mig1 and therefore its nucleocytoplasmic distribution. *J Biol Chem* **282:** 4485-4493

De Vit MJ, Waddle JA, Johnston M (1997) Regulated nuclear translocation of the Mig1 glucose repressor. *Mol Biol Cell* **8:** 1603-1618

Gasch AP, Spellman PT, Kao CM, Carmel-Harel O, Eisen MB, Storz G, Botstein D, Brown PO (2000) Genomic expression programs in the response of yeast cells to environmental changes. *Mol Biol Cell* **11:** 4241-4257

Hong SP, Leiper FC, Woods A, Carling D, Carlson M (2003) Activation of yeast Snf1 and mammalian AMP-activated protein kinase by upstream kinases. *Proc Natl Acad Sci U S A* **100:** 8839-8843

O'Farrell PH (1975) High resolution two-dimensional electrophoresis of proteins. *J Biol Chem* **250:** 4007-4021

Sutherland CM, Hawley SA, McCartney RR, Leech A, Stark MJ, Schmidt MC, Hardie DG (2003) Elm1p is one of three upstream kinases for the Saccharomyces cerevisiae SNF1 complex. *Curr Biol* **13:** 1299-1305

Yellman CM, Burke DJ (2004) Assaying the spindle checkpoint in the budding yeast Saccharomyces cerevisiae. *Methods Mol Biol* **280:** 275-290